

Electronic Supplementary Material (ESI) for Faraday Discussions.
This journal is © The Royal Society of Chemistry 2021

Density functional theory investigation of Ru(II) and Os(II) asymmetric transfer hydrogenation catalysts

Elizabeth M. Bolitho^[a], James P. C. Coverdale^[b], Juliusz A. Wolny^{[c]*}, Volker Schünemann^[c], Peter J. Sadler^{[a]*}

^[a] Department of Chemistry, University of Warwick, Coventry, CV4 7AL UK

^[b] School of Pharmacy, Institute of Clinical Sciences, University of Birmingham, Edgbaston, B15 2TT

^[c] Fachbereich Physik, Technische Universität Kaiserslautern, Kaiserslautern, Germany

*Corresponding authors: p.j.sadler@warwick.ac.uk and wolny@physik.uni-kl.de

| Contents | |
|---|-----|
| PDB structures | S3 |
| Diamine ligand nomenclature | S4 |
| Chirality assignment | S5 |
| References for guidelines on chirality assignment | S9 |
| Figure S1. Structure of the transition state for inversion of the axial chirality of [Os/Ru(η^6 - <i>p</i> -cymene)(TsDPEN-H)H] | S9 |
| Figure S2. Structure of the <i>R</i> -configured hydride complex [<i>R</i> -Ru(<i>p</i> -cymene)(<i>S,S</i> -TsDPEN-H)-H] (with <i>R</i> metal chirality, <i>S_a</i> or <i>R_a</i> axial chirality, and <i>S,S</i> ligand chirality), showing the π - π interaction between the phenyl of acetophenone and the tosyl group of the catalyst. | S10 |
| Figure S3. Model for the interaction of the C=O group of acetophenone with [Ru(η^6 - <i>p</i> -cymene)(TsDPEN-H)H] bearing <i>R</i> metal chirality, (<i>S,S</i>) ligand chirality, and <i>R_a</i> axial chirality. | S11 |
| Figure S4. [<i>R</i> -M(<i>p</i> -cymene)(<i>S,S</i> -TsDPEN-H)H] with metal = <i>R</i> , diamine= <i>S,S</i> , axial = <i>S_a</i> (shown in Figure 3a). Cf. PDB1. | S12 |
| Figure S5. [<i>R</i> -M(<i>p</i> -cymene)(<i>S,S</i> -TsDPEN-H)H] with metal = <i>R</i> , diamine= <i>S,S</i> , axial = <i>R_a</i> (shown in Figure 3b) Cf. PDB2. | S12 |
| Figure S6. Transition state between [<i>R</i> -M(<i>p</i> -cymene)(<i>S,S</i> -TsDPEN-H)H] with metal = <i>R</i> , diamine= <i>S,S</i> , axial = <i>R_a</i> / <i>S_a</i> (shown in Figure S1 of supplementary Information) Cf. PDB3 | S12 |
| Figure S7 [M(η^6 - <i>p</i> -cymene)(TsDPEN-H)H] where metal = <i>R</i> , diamine = <i>S,S</i> showing η^6 coordination (shown in Figure 4a) (the same as PDB1) Cf. PDB4 | S12 |
| Figure S8 [M(η^6 - <i>p</i> -cymene)(TsDPEN-H)H] where metal = <i>S</i> , diamine = <i>S,S</i> showing η^2 coordination (shown in Figure 4b) Cf. PDB5 | S13 |
| Figure S9 [<i>R</i> -Ru(<i>p</i> -cymene)(<i>S,S</i> -TsDPEN-H)H] metal= <i>R</i> , diamine = <i>S,S</i> , axial = <i>R_a</i> with acetophenone and CO ₂ (shown in Figure S2) Cf. PDB6 | S13 |
| Figure S10 Species A for ruthenium (shown in Figure 5) for <i>S_a</i> Cf. PDB7 | S13 |
| Figure S11 Species A for ruthenium (shown in Figure 5) for <i>R_a</i> Cf. PDB8 | S13 |
| Figure S12 Species B for ruthenium (shown in Figure 5) for <i>S_a</i> Cf. PDB9 | S14 |
| Figure S13 Species B for ruthenium (shown in Figure 5) for <i>R_a</i> Cf. PDB10 | S14 |
| Figure S14 Species C for ruthenium (shown in Figure 5) for <i>S_a</i> Cf. PDB11 | S14 |
| Figure S15 Species C for ruthenium (shown in Figure 5) for <i>R_a</i> Cf. PDB12 | S14 |
| Figure S16 Species D for ruthenium (shown in Figure 5) for <i>R_a</i> Cf. PDB13 | S15 |

| | |
|---|-----|
| Figure S17 Species E for ruthenium (shown in Figure 5) for R_a (<i>R</i> -phenylethanol) with energy 7 kJ/mol Cf. PDB14 | S15 |
| Figure S18 Species E for ruthenium (shown in Figure 5) for R_a (<i>S</i> -phenylethanol) with energy 26 kJ/mol Cf. PDB15 | S15 |
| Figure S19 Species A for osmium (shown in Figure 7) for S_a Cf. PDB16 | S16 |
| Figure S20 Species A for osmium (shown in Figure 7) for R_a Cf. PDB17 | S16 |
| Figure S21 Species B for osmium (shown in Figure 7) for S_a Cf. PDB18 | S16 |
| Figure S22 Species B for osmium (shown in Figure 7) for R_a Cf. PDB19 | S16 |
| Figure S23 Species C for osmium (shown in Figure 7) for S_a Cf. PDB20 | S17 |
| Figure S24 Species C for osmium (shown in Figure 7) for R_a Cf. PDB21 | S17 |
| Figure S25 Species D for osmium (shown in Figure 7) for R_a Cf. PDB22 | S17 |
| Figure S26 Species E for osmium (shown in Figure 7) for R_a with energy 7 k/mol Cf. PDB23 | S18 |
| Figure S27 Species E for osmium (shown in Figure 7) for R_a with energy 26 k/mol Cf. PDB24 | S18 |
| Figure S28 Another conformer of the [Ru(<i>p</i> -cymene)(<i>S,S</i> -TsDPEN-H)] / acetophenone assembly with the CO \cdots HN hydrogen bonding (denoted with the dashed line). (shown in Figure 10) Cf. PDB25 | S18 |
| Figure S29 Species (iii) in Figure 11 Cf. PDB26 | S19 |
| Figure S30 Species (iv) in Figure 11. An estimated transition state of the hydride transfer, corresponding to the structure in middle in Fig. 9 Cf. PDB27 | S19 |
| Figure S31 Species (v) in Figure 11 Cf. PDB28 | S19 |

PDB structures

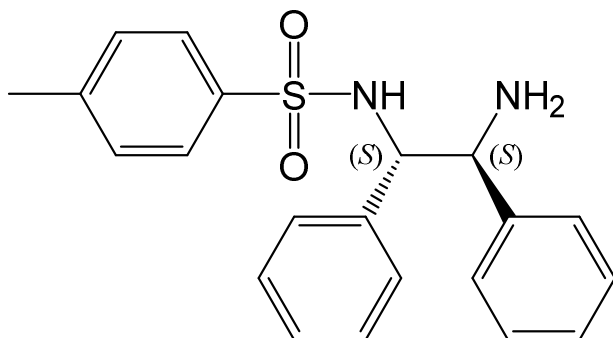
Calculated structures described in this work have been submitted alongside the manuscript as PDB files. The Table below describes the filename of the PDB file and a brief description of the structure. The corresponding structures are shown in Figs S4-S31,

| PDB file | Description |
|----------|---|
| PDB1 | [R-M(<i>p</i> -cymene)(<i>S,S</i> -TsDPEN-H)H] with metal = R, diamine= <i>S,S</i> , axial = S_a (shown in Figure 3a) |
| PDB2 | [R-M(<i>p</i> -cymene)(<i>S,S</i> -TsDPEN-H)H] with metal = R, diamine= <i>S,S</i> , axial = R_a (shown in Figure 3b) |
| PDB3 | Transition state between [R-M(<i>p</i> -cymene)(<i>S,S</i> -TsDPEN-HH)] with metal = R, diamine= <i>S,S</i> , axial = R_a / S_a (shown in Figure S1 of the ESI) |
| PDB4 | [M(η^6 - <i>p</i> -cymene)(TsDPEN-H)H] where metal = R, diamine = <i>S,S</i> showing η^6 coordination (shown in Figure 4a) (the same as PDB1) |
| PDB5 | [M(η^6 - <i>p</i> -cymene)(TsDPEN-H)H] where metal = S, diamine = <i>S,S</i> showing η^2 coordination (shown in Figure 4b) |
| PDB6 | [R-Ru(<i>p</i> -cymene)(<i>S,S</i> -TsDPEN-H)H] metal=R, diamine = <i>S,S</i> , axial = R_a with acetophenone and CO ₂ (shown in Figure S2) |
| PDB7 | Species A for ruthenium (shown in Figure 5) for S_a |
| PDB8 | Species A for ruthenium (shown in Figure 5) for R_a |
| PDB9 | Species B for ruthenium (shown in Figure 5) for S_a |
| PDB10 | Species B for ruthenium (shown in Figure 5) for R_a |
| PDB11 | Species C for ruthenium (shown in Figure 5) for S_a |
| PDB12 | Species C for ruthenium (shown in Figure 5) for R_a |
| PDB13 | Species D for ruthenium (shown in Figure 5) for R_a |
| PDB14 | Species E for ruthenium (shown in Figure 5) for R_a (<i>R</i> -phenylethanol) with energy 7 kJ/mol |
| PDB15 | Species E for ruthenium (shown in Figure 5) for R_a (<i>S</i> -phenylethanol) with energy 26 kJ/mol |
| PDB16 | Species A for osmium (shown in Figure 7) for S_a |
| PDB17 | Species A for osmium (shown in Figure 7) for R_a |
| PDB18 | Species B for osmium (shown in Figure 7) for S_a |
| PDB19 | Species B for osmium (shown in Figure 7) for R_a |
| PDB20 | Species C for osmium (shown in Figure 7) for S_a |
| PDB21 | Species C for osmium (shown in Figure 7) for R_a |
| PDB22 | Species D for osmium (shown in Figure 7) for R_a |
| PDB23 | Species E for osmium (shown in Figure 7) for R_a with energy 7 k/mol |
| PDB24 | Species E for osmium (shown in Figure 7) for R_a with energy 26 k/mol |
| PDB25 | Another conformer of the [Ru(<i>p</i> -cymene)(<i>S,S</i> -TsDPEN-H)] / acetophenone assembly with the CO \cdots HN hydrogen bonding (denoted with the dashed line). (shown in Figure 10) |
| PDB26 | Species (iii) in Figure 11 |
| PDB27 | Species (iv) in Figure 11. An estimated transition state of the hydride transfer, corresponding to the structure in middle of Fig. 9 |
| PDB28 | Species (v) in Figure 11 |

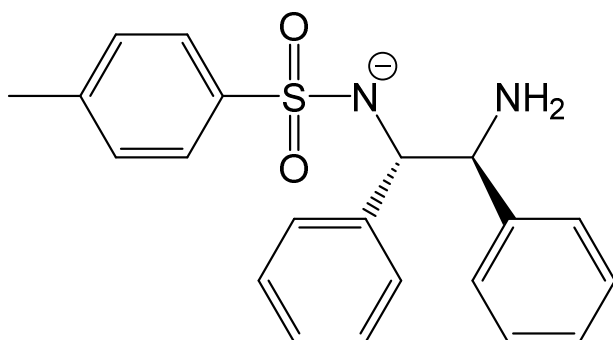
Diamine ligand nomenclature

Nomenclature of the tosyl diamine ligand (*S,S*)-1,2-*N*-tosyl-diphenylethylenediamine has been included with the following designation of ligand protonation (anionic charge). Note that all diamine ligands in this work are of absolute configuration (*S,S*).

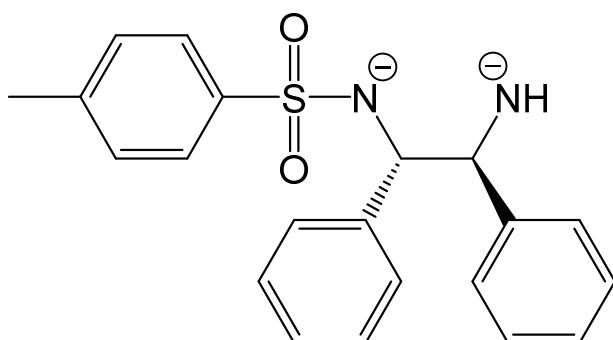
TsDPEN 1,2-*N*-tosyl-diphenylethylenediamine (neutral species)



TsDPEN-H Deprotonation of the nitrogen adjacent to tosyl (L^- anionic species)



TsDPEN-H₂ Deprotonation of both nitrogen atoms (L^{2-} dianionic species)



Chirality assignment

There are four elements of chirality in the hydride complexes under study:

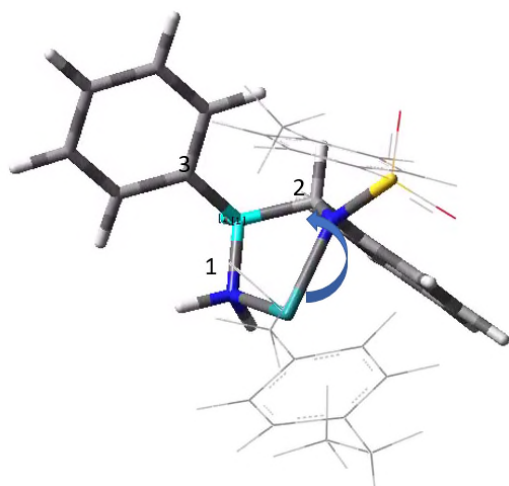
1. Chirality of the chelate carbon atoms
2. Metal chirality
3. Axial chirality of the cymene bound to metal
4. Chirality of the chelate ring

1. Chirality of the chelate ring carbons

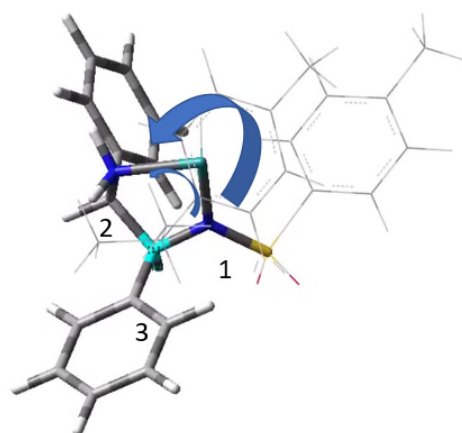
The hydride complex showing chiral carbon ligand atoms is shown. In the case of the chelate ring carbons in the hydride complex, N bound to S (in the tosylate, Ts) has highest priority, followed by N bound to C. Of the two carbon atoms, one is bound to NH₂, the other one is bound to NTs. The following CIP priorities can be assigned (from lowest to highest):

1. **H** (1 – lowest priority)
2. **C-NH₂** (12, 12, 14 – N is attached to protons only)
3. **C-NTs** (12, 12, 14 – N is attached to tosylate sulphur)
4. **N** (14 – highest priority)

The two chiral carbons are shown highlighted in cyan. The hydrogen is pointing behind the plane of the figure. The numbers display the priorities of the bound atoms. Hence, the configuration of both chelate ring carbons are *S*.



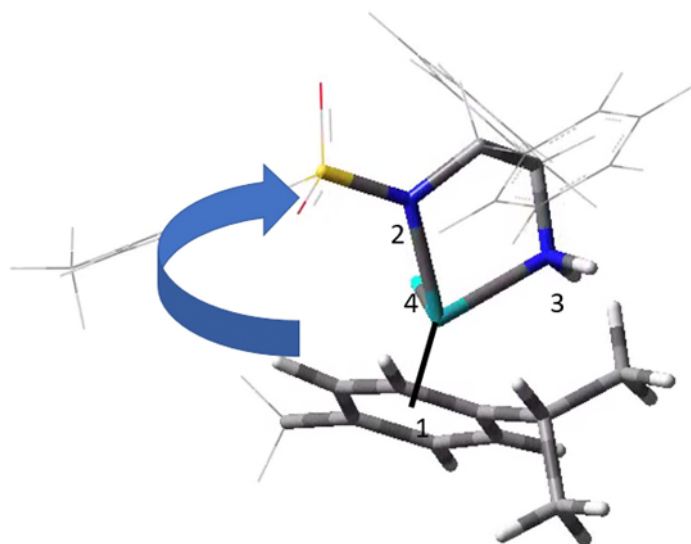
Anticlockwise, (*S*)



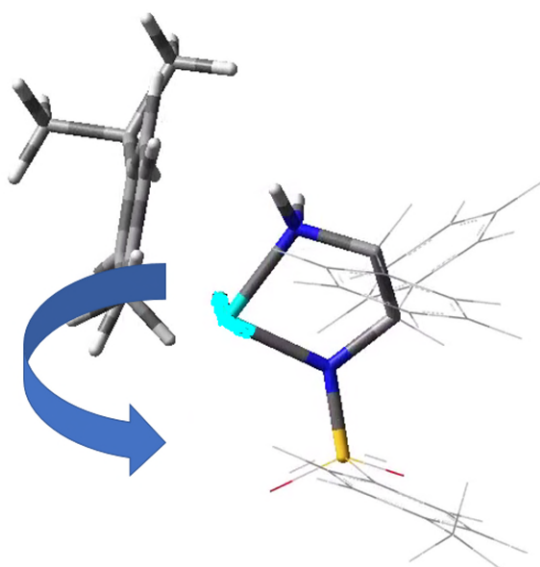
Anticlockwise, (*S*)

2. Metal chirality

In this case we treat the metal as tetrahedrally-coordinated. The arene has the highest priority (6 x 12, following the convention suggested by Lecomte *et al.*, and Stanley and Baird) followed by N bound to S, N bound to C, and then hydride, the lowest priority.^{3,4} Thus, there are two enantiomers differing in the absolute configuration of the metal.



Clockwise, (*R*)

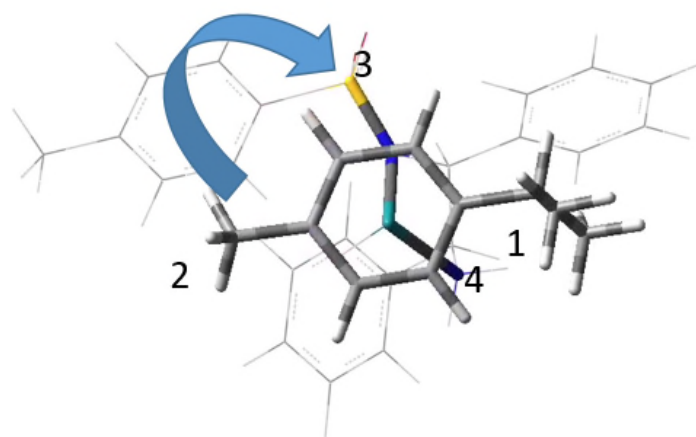


Anticlockwise, (*S*)

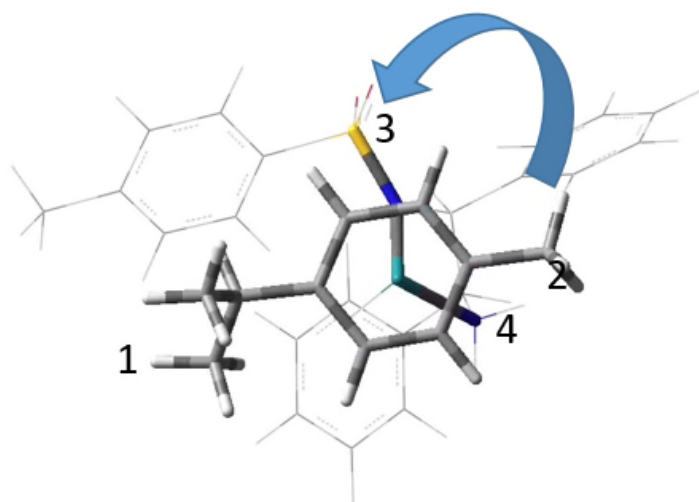
3. Axial chirality

We consider two atropisomers due to η^6 -*p*-cymene rotation around the M-(η^6 -*p*-cymene) bond. While the *N,N'* chelate does not have the symmetry plane there are two possible rotamers characterised by axial chirality descriptors. Four groups given below according to decreasing priority define the chirality; hence, there are two enantiomers of different axial chirality:

1. ***i*Pr** (in the forward plane)
2. **Me** (in the forward plane)
3. **NTs** (behind the plane)
4. **NH₂** (behind the plane)



R_a axial chirality



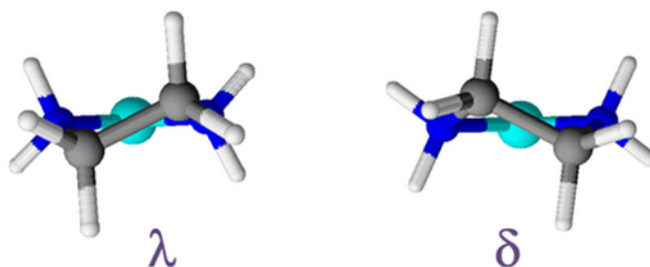
S_a axial chirality

4. Chelate ring chirality

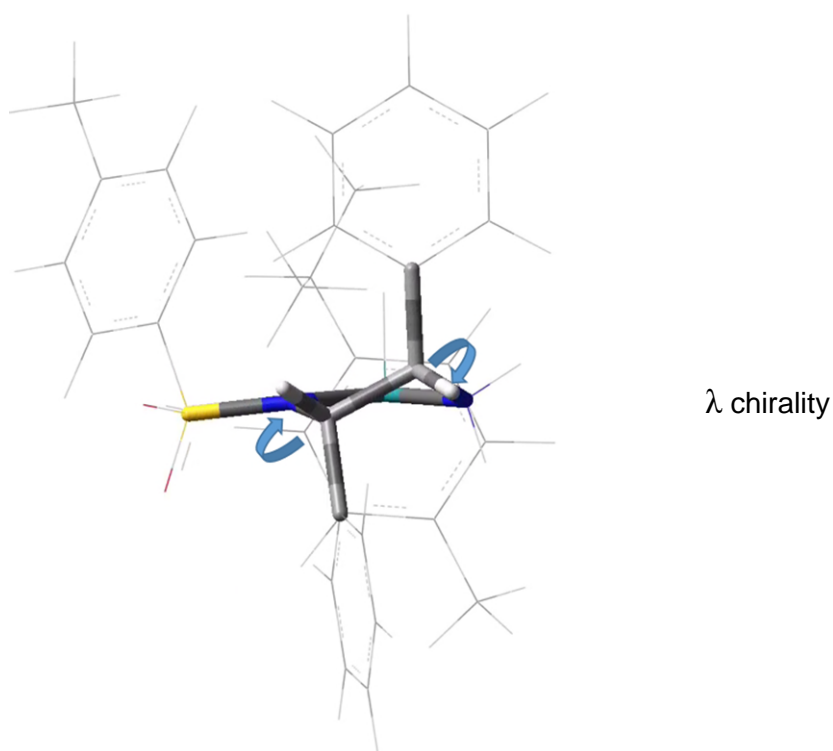
To understand the two most stable conformers of five-membered chelates rings, it is helpful to think of five-membered chelate rings as involving two components:

- a planar L-M-L group, where L are the atoms directly attached to the metal, M
- the remaining two ring atoms, E, which form a rigid E-E bar across the back of the chelate ring^{5,6}

λ chirality is the movement from the closer atom to its neighbour behind is clockwise. It is anticlockwise for δ .



Inspection of the optimised structures shows that all have λ chirality as shown below:



References for guidelines on chirality assignment

Organic compounds

1. E.L. Eliel, S. H. Wilen, Stereochemistry of organic compounds, *John Wiley & Sons, Inc.*, 1994, ISBN 0-471-01670-5

Inorganic complexes

2. R. Kramer, Stereochemistry of Coordination Compounds, *John Wiley & Sons Inc.*, 1996, ISBN 0-471-95057-2

Organometallic arene complexes

3. C. Lecomte, *et al.*, *J. Organomet. Chem.* 1974, **73**, 67.
4. K. Stanley, M. C. Baird, *J. Am. Chem. Soc.* 1975, **97**, 6598.

For chelate ring chirality

5. C. J. Hawkins, Absolute Configuration of Metal Complexes, Wiley Interscience, New York, 1971
6. J. Beattie, *Acc. Chem. Res.* 1971, **4**, 253.

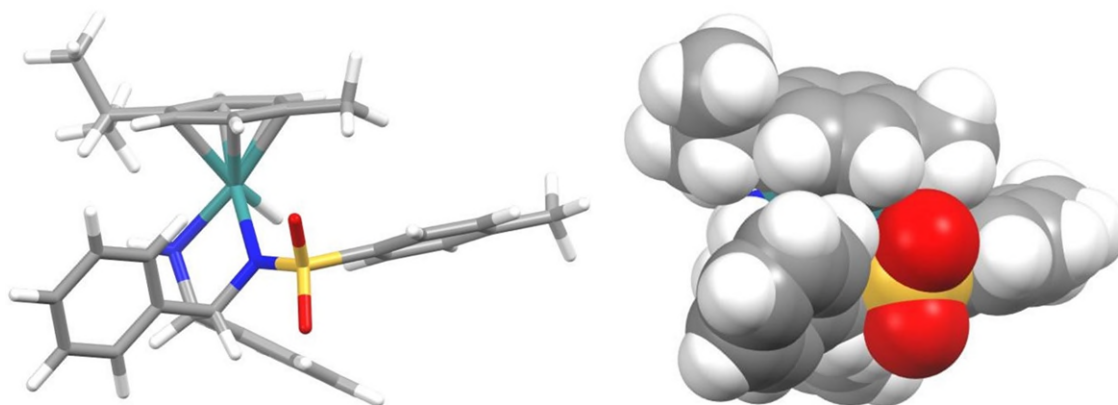
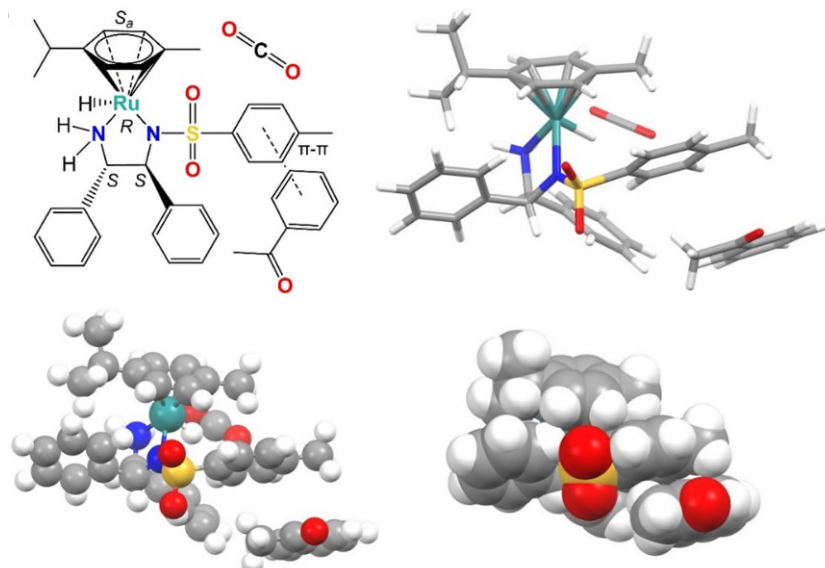


Figure S1. Structure of the transition state for inversion of axial chirality of [M(*p*-cymene)(TsDPEN-H)H]. The energy barrier for *p*-cymene rotation is $> 20 \text{ kJ mol}^{-1}$ between S_a and R_a . See **PDB3**.

(a) Metal = *R*, diamine = *S,S*, axial = *S_a*



(b) Metal = *R*, diamine = *S,S*, axial = *R_a*

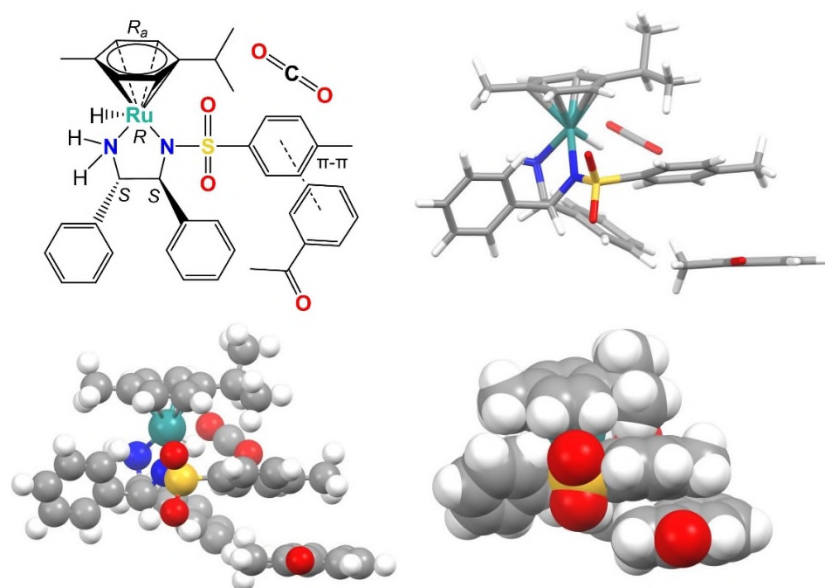
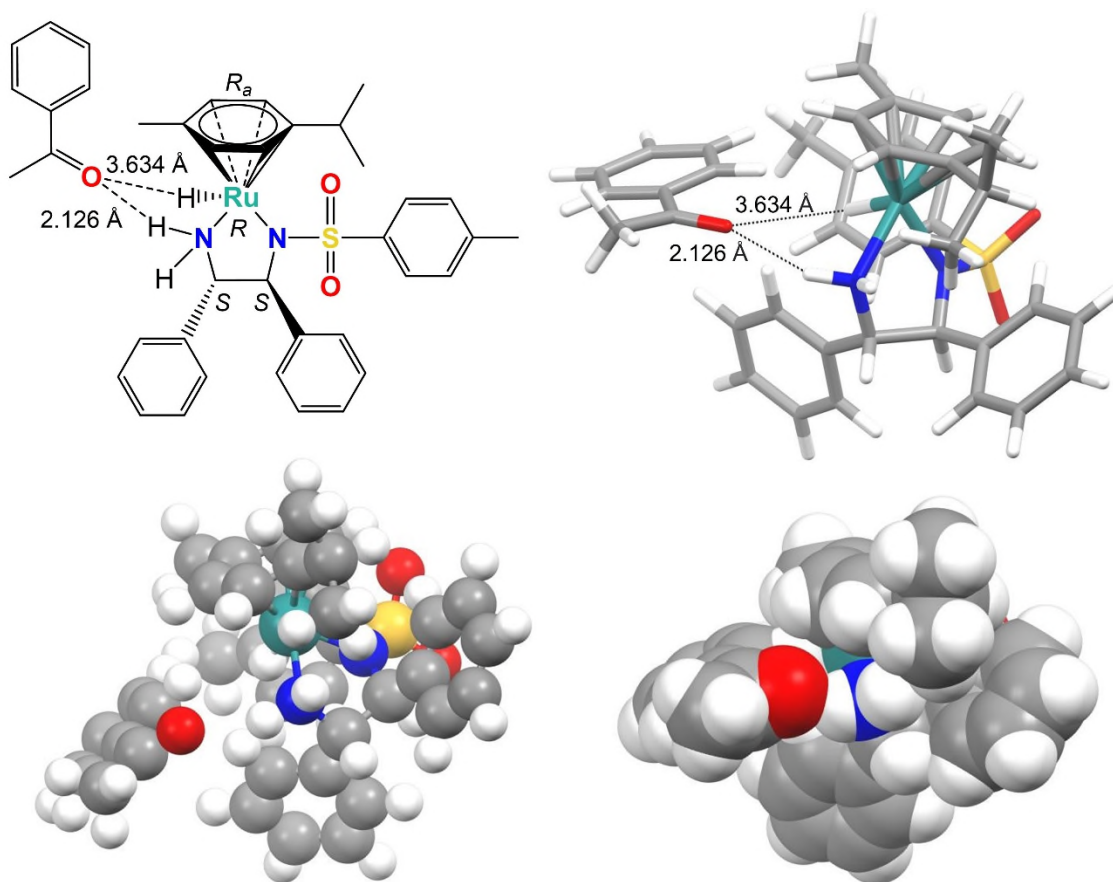


Figure S2. Structure of the *R*-configured hydride complex [*R*-Ru(p-cymene)(*S,S*-TsDPEN-H)-H] (with *R* metal chirality, *S_a* or *R_a* axial chirality, and *S,S* ligand chirality), showing the π-π interaction between the phenyl of acetophenone and the tosyl group of the catalyst. Notably, there is a significant interaction of the formed CO₂ molecule with Ru-H, with a H...C distance of *ca.* 2.6 Å. See **PDB6**.



Metal = *R*, diamine = (*S,S*), axial = *R_a*

Figure S3. Model for the interaction of the C=O group of acetophenone with [Ru(η^6 -*p*-cymene)(TsDPEN-H)H] with *R* metal chirality, *R_a* axial chirality and (*S,S*) ligand chirality. The (acetophenone) carbonyl oxygen C=O \cdots H₂N (catalyst) distance is 2.126 Å, and the (acetophenone) carbonyl oxygen C=O \cdots H-N (catalyst) distance is 3.634 Å. See **PDB25**.

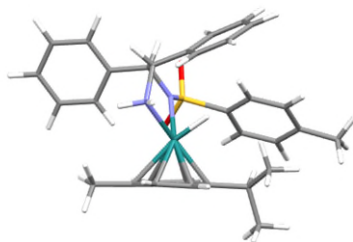


Figure S4. $[R\text{-M}(p\text{-cymene})(S,S\text{-TsDPEN-H})\text{H}]$ with metal = *R*, diamine = *S,S*, axial = *S_a* (shown in Figure 3a). Cf. **PDB1**.

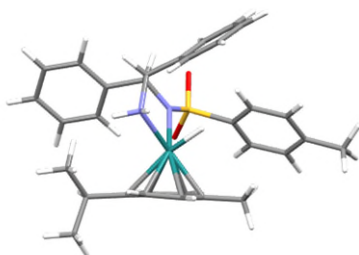


Figure S5. $[R\text{-M}(p\text{-cymene})(S,S\text{-TsDPEN-H})\text{H}]$ with metal = *R*, diamine = *S,S*, axial = *R_a* (shown in Figure 3b). Cf. **PDB2**.

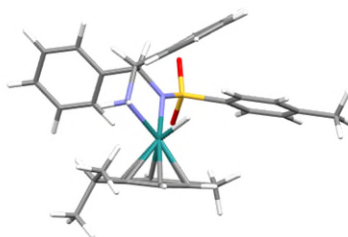


Figure S6. Transition state between $[R\text{-M}(p\text{-cymene})(S,S\text{-TsDPEN-H})\text{H}]$ with metal = *R*, diamine = *S,S*, axial = *R_a* / *S_a* (shown in Figure S1 of supplementary Information). Cf. **PDB3**.

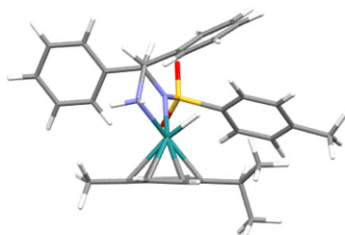


Figure S7 $[\text{M}(\eta^6\text{-}p\text{-cymene})(\text{TsDPEN-H})\text{H}]$ where metal = *R*, diamine = *S,S* showing η^6 coordination (shown in Figure 4a) (the same as PDB1). Cf. **PDB4**.

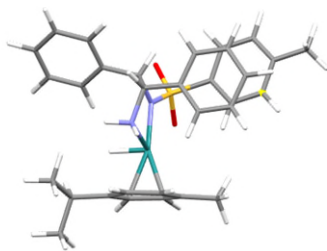


Figure S8 [M(η^6 -*p*-cymene)(TsDPEN-H)H] where metal = *S*, diamine = *S,S* showing η^2 coordination (shown in Figure 4b). Cf. **PDB5**.

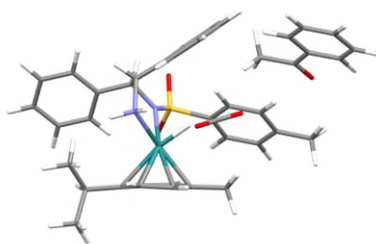


Figure S9 [*R*-Ru(*p*-cymene)(*S,S*-TsDPEN-H)H] metal=*R*, diamine = *S,S*, axial = *R_a* with acetophenone and CO₂(shown in Figure S2). Cf. **PDB6**.

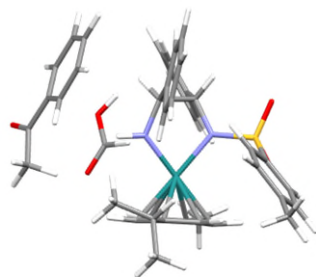


Figure S10 Species **A** for ruthenium (shown in Figure 5) for *S_a*. Cf. **PDB7**.

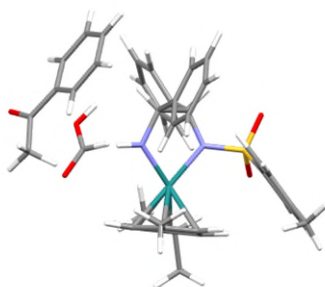


Figure S11 Species **A** for ruthenium (shown in Figure 5) for *R_a*. Cf. **PDB8**.

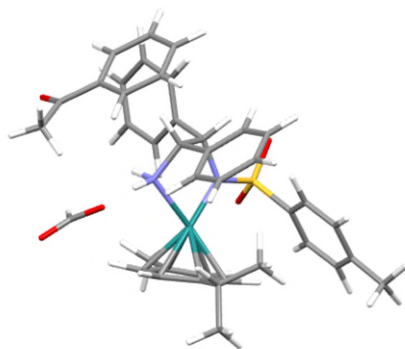


Figure S12 Species **B** for ruthenium (shown in Figure 5) for S_a . Cf. **PDB9**.

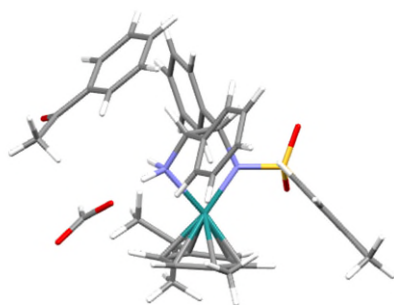


Figure S13 Species **B** for ruthenium (shown in Figure 5) for R_a . Cf. **PDB10**.

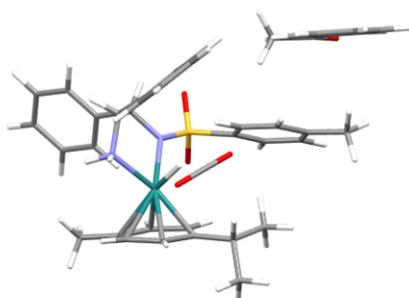


Figure S14 Species **C** for ruthenium (shown in Figure 5) for S_a . Cf. **PDB11**.

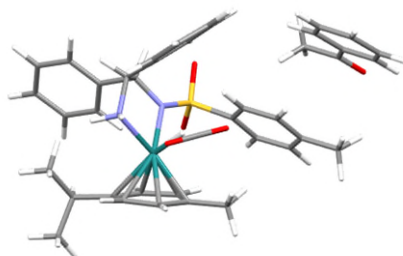


Figure S15 Species **C** for ruthenium (shown in Figure 5) for R_a . Cf. **PDB12**.

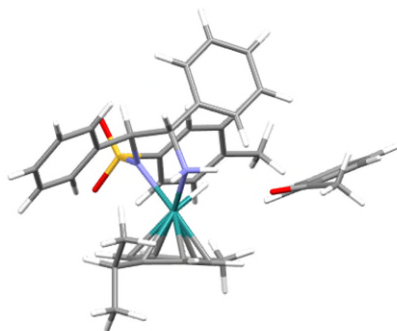


Figure S16 Species **D** for ruthenium (shown in Figure 5) for R_a . Cf. **PDB13**. The remote CO_2 molecule is not shown.

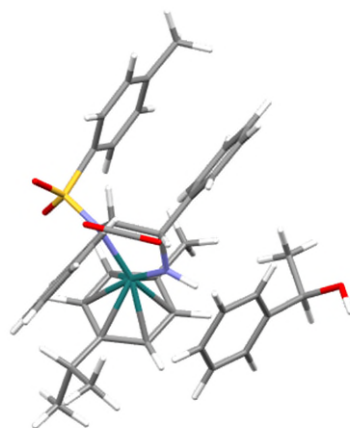


Figure S17 Species **E** for ruthenium (shown in Figure 5) for R_a (*R*-phenylethanol) with energy 7 kJ/mol. Cf. **PDB14**.

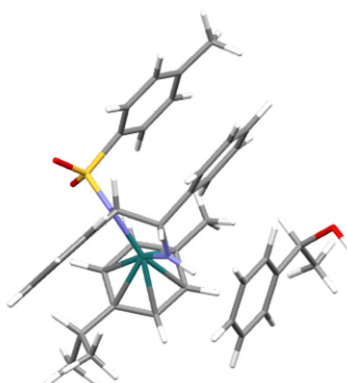


Figure S18 Species **E** for ruthenium (shown in Figure 5) for R_a (*S*-phenylethanol) with energy 26 kJ/mol. Cf. **PDB15**. The remote CO_2 molecule is not shown.

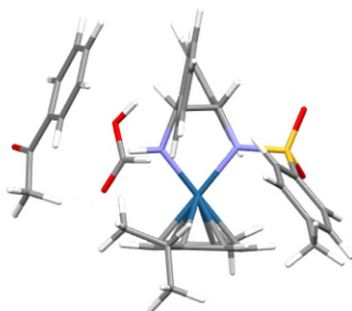


Figure S19 Species **A** for osmium (shown in Figure 7) for S_a . Cf. **PDB16**

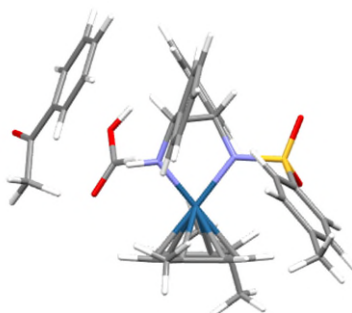


Figure S20 Species **A** for osmium (shown in Figure 7) for R_a . Cf. **PDB17**.

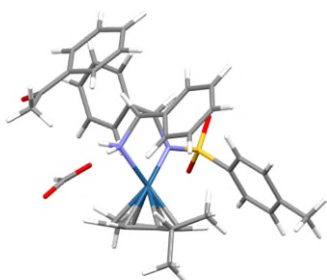


Figure S21 Species **B** for osmium (shown in Figure 7) for S_a . Cf. **PDB18**.

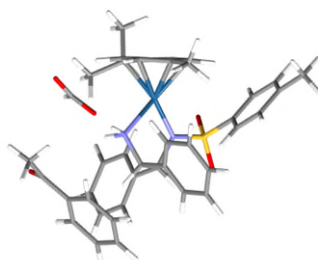


Figure S22 Species **B** for osmium (shown in Figure 7) for R_a . Cf. **PDB19**.

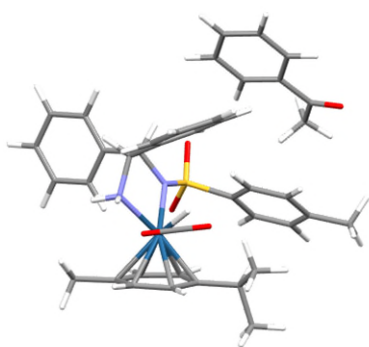


Figure S23 Species **C** for osmium (shown in Figure 7) for S_a . Cf. **PDB20**.

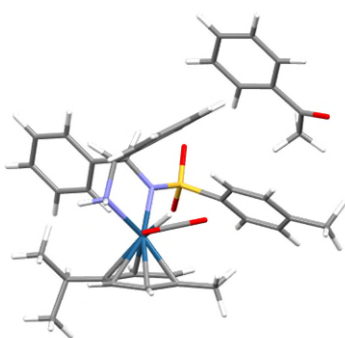


Figure S24 Species **C** for osmium (shown in Figure 7) for R_a . Cf. **PDB21**

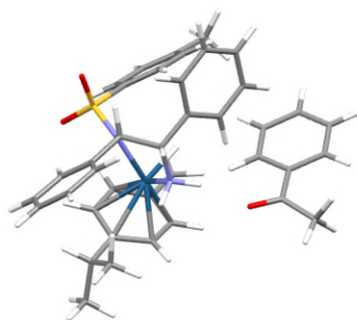


Figure S25 Species **D** for osmium (shown in Figure 7) for R_a . Cf. **PDB22**

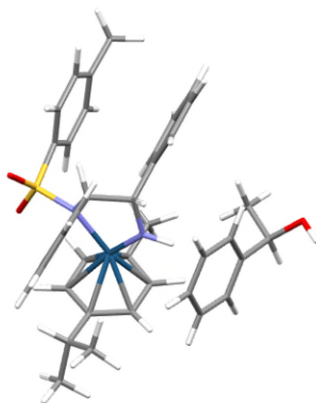


Figure S26 Species **E** for osmium (shown in Figure 7) for R_a with energy 7 kJ/mol. Cf. **PDB23**. The remote CO_2 molecule is not shown.

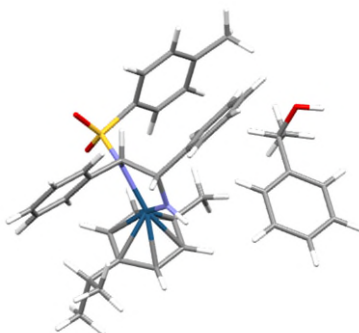


Figure S27 Species **E** for osmium (shown in Figure 7) for R_a with energy 26 kJ/mol. Cf. **PDB24**. The remote CO_2 molecule is not shown.

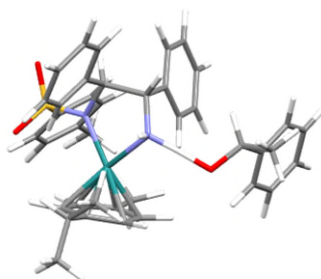


Figure S28 Species (iv) in Figure 11. An estimated transition state of the hydride transfer, corresponding to the structure in middle in Fig. 9. Cf. **PDB25**. The remote CO_2 molecule is not shown.

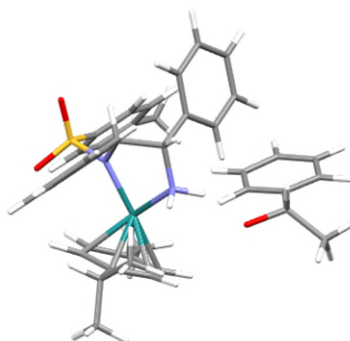


Figure S29 Species (iii) in Figure 11 Cf. **PDB26**. The remote CO_2 molecule is not shown.

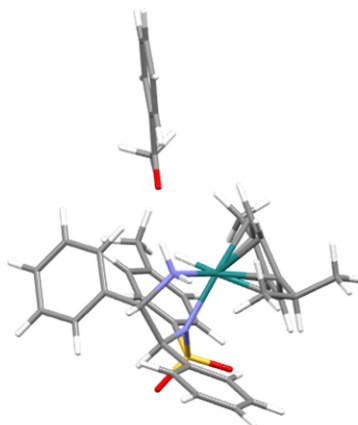


Figure S30 Another conformer of the [Ru(p-cymene)(S,S-TsDPEN-H)] / acetophenone assembly with the CO \cdots HN hydrogen bonding (denoted with the dashed line). (shown in Figure 10). Cf. **PDB27**. The remote CO₂ molecule is not shown.

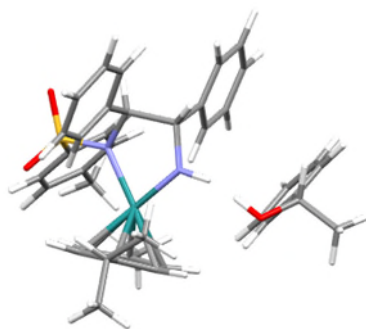


Figure S31 . Species (v) in Fig 11. Cf. **PDB28**. Remote CO₂ molecule is not shown.